BOLETIN DE LA SOCIEDAD ESPAÑOLA DE
Cerámica y Vidrio
A R T I C U L O

Influence of alumina characteristics on glaze properties

E. BOU[(1)], J. GARCÍA-TEN[(1)], R. PÉREZ[(1)], S. ARRUFAT[(1)], G. ATICHIAN[(2)]

[(1)] Instituto de Tecnología Cerámica (ITC). Asociación de Investigación de las Industrias Cerámicas (AICE). Universitat Jaume I. Castellón. Spain.
[(2)] RIO TINTO ALCAN, Specialty Aluminas. Gardanne. France

Este trabajo ha sido presentado como comunicación oral en el XI World Congress on Ceramic Tile Qualicer. (Castellón, España, 2010)

Aluminium oxide is a synthetic raw material manufactured from bauxite by the Bayer process, whose Al_2O_3 content typically exceeds 99%. Four main types of alumina can be defined, depending on the processing used: hydrargillite $Al(OH)_3$, boehmite AlOOH, transition aluminas (calcined at low temperatures, 1000 °C, with an intermediary crystallographic structure between hydrates and alpha alumina), and α-Al_2O_3 (calcined at high temperatures, >1100 °C). In glaze manufacturing, α-Al_2O_3 is the main type of alumina used. This raw material acts as a matting agent: the matt effect depends on alumina particle size and content in the glaze. This study examines the effect of the degree of alumina calcination on glaze technical and aesthetic properties. For this purpose, aluminas with different degrees of calcination were added to a glaze formulated with a transparent frit and kaolin, in order to simplify the system to be studied. The results show that, depending on the degree of calcination, alumina particles can react with the glaze components (SiO_2, CaO, and ZnO) to form new crystalline phases (anorthite and gahnite). Both crystallisations extract CaO and ZnO from the glassy phase, increasing glassy phase viscosity. The variation in crystalline phases and glassy phase viscosity yields glazes with different technical and aesthetic properties.

Keywords: Glaze, alumina, degree of calcination.

Influencia de las características de la alúmina en las propiedades del esmalte

El óxido de aluminio es una materia prima sintética fabricada a partir de la bauxita por medio del proceso Bayer, cuyo contenido de Al_2O_3 supera, por regla general, el 99%. Se pueden definir cuatro tipos de alúmina, en función del tipo de proceso usado: hidrargilita $Al(OH)_3$, boehmita AlOOH, alúminas de transición (calcinadas a bajas temperaturas, 1000 °C, con una estructura cristalográfica intermedia entre los hidratos y la alfa alúmina), y la α-Al_2O_3 (calcinada a altas temperaturas, >1100 °C). En la fabricación de los esmaltes, α-Al_2O_3 es el tipo principal de alúmina usado. Esta materia prima actúa como matificante: el efecto mate depende del tamaño de la partícula de alúmina y de su contenido en el esmalte. Este estudio examina el efecto del grado de calcinación de la alúmina en las propiedades estéticas y técnicas del esmalte. Para esto, se han añadido alúminas con distintos grados de calcinación al esmalte formulado con una frita transparente y caolín, para simplificar el sistema a estudiar. Los resultados demuestran que, en función del grado de calcinación, las partículas de alúmina pueden reaccionar con los componentes del esmalte (SiO_2, CaO, y ZnO) para formar nuevas fases cristalinas (anortita y gahnita). Ambas cristalizaciones extraen CaO y ZnO de la fase vítrea, incrementando la viscosidad de la fase vítrea. La variación de las fases cristalinas y la viscosidad de la fase vítrea generan vidriados con propiedades técnicas y estéticas distintas.

Palabras clave: Esmalte, alúmina, grado de calcinación.

1. INTRODUCTION

Alumina is a synthetic raw material manufactured from bauxite by the Bayer process, whose Al_2O_3 content is typically higher than 99%. The process involves, among other phases, a Na(OH) chemical attack phase in which hydrates form and a calcination phase, in rotary kilns, in which the hydrates are transformed into transition aluminas and alpha alumina (α-Al_2O_3). As a result, alumina exists in different physical and chemical forms. Four main types of alumina compounds can be defined, depending on the processing used: hydrargillite $Al(OH)_3$, boehmite AlOOH, transition aluminas (calcined at low temperatures, 1000 °C, with an intermediary crystallographic structure between hydrates and alpha alumina), and α-Al_2O_3 (calcined at high temperatures, >1100 °C) [1][2].

During the calcination process, the specific surface area (SSA) of the alumina decreases with increasing temperature. For this reason, alumina SSA is typically used to evaluate the alumina degree of calcination. Transition aluminas have a higher SSA than α-Al_2O_3.

In tile manufacturing, α-Al_2O_3 is the main type of alumina used in bodies and glazes [3][4][5]. This raw material acts as an opacifier in porcelain tiles and as a matting agent in glazes [6][7][8][9]. In this last case, the matt effect depends on alumina particle size and content in the glaze. The refractory behaviour of the alumina provides a glass matrix with undissolved particles that hinder the obtainment of smooth surfaces.

This study has been undertaken to examine how different types of alumina affect the technical and aesthetic properties of the resulting glaze. For this purpose, aluminas with different

degrees of calcination were added to a glaze formulated with a transparent frit and kaolin, in order to simplify the system to be studied.

2. EXPERIMENTAL

2.1 Materials

The study was conducted using four alumina samples with different degrees of calcination, DC (Table I). The degree of calcination was estimated based on the specific surface area (SSA) of each sample.

These aluminas were introduced into a glaze composition used in industry to produce transparent and glossy glazes. This glaze contains frit and kaolin, whose chemical compositions are shown in Table II.

2.2 Glaze suspension preparation

The glaze suspension was prepared by wet milling the raw materials blend at 70% solids content by weight in a laboratory mill with alumina balls. The mixture was milled until a reject of about 1 wt% was obtained on a 40-μm mesh screen. The raw materials blend consisted of:

Solids (% by weight): 80% frit, 7% kaolin, and 13% alumina

Additives (% by weight relative to the solid): 0.3% sodium carboxymethylcellulose and 0.3% sodium tripolyphosphate

To determine the effect of the alumina in the glaze, a glaze without alumina, referenced the STD glaze, was also prepared.

2.3 Glaze characterisation

The glaze suspensions were applied on to red-firing wall tile bodies, with and without engobe. The applied glaze layer had a thickness of 500 μm. The glazed specimens were dried in an electric laboratory oven at 110 ºC and subsequently fired in an electric laboratory kiln. The following peak temperatures were tested: 1080, 1100, 1120, and 1140 ºC.

TABLE I. ALUMINA PROPERTIES

Ref.	d_{50} (μm)	SSA (m^2/g)	DC
AC28	45	0.31	High
AC34	59	0.56	High
AR308	76	7.1	Low
AR75	105	75	Low

GLAZE AESTHETIC CHARACTERISTICS

Opacity

The colour of non-engobed glazed tiles is related to glaze opacity [10]. The chromatic co-ordinates (L*, a*, and b*) of the fired glazed specimens were determined on a spectrophotometer that performs the measurements according to the CIE Lab system, using a C light source and CIE 2º standard observer.

Colour and gloss

These properties were determined on the engobed glazed tiles. The whiteness and yellowness indexes (WI: whiteness index HUNTER [60], YI: yellowness index ASTM D1925) were measured on a spectrophotometer, as described in the glaze opacity test. Surface gloss was determined on a glossmeter, measuring at an angle of 60º.

MICROSTRUCTURAL CHARACTERISATION

Identification of crystalline phases

The crystalline phases were identified by X-ray diffraction in unfired samples of powdered glaze and in powdered glaze samples fired at 1120 ºC.

Observation by scanning electron microscopy (SEM)

Glazed tiles with engobe obtained at 1120 ºC were observed by SEM. Two types of observations were performed, one of the surface and another of the polished cross-section. All the test specimens were observed with a scanning electron microscope coupled to an energy-dispersive X-ray microanalysis (EDXA) instrument.

Glaze porosity

A cross-section of the glaze layers was observed by optical microscope to evaluate glaze porosity.

GLAZE TECHNICAL PROPERTIES

Chemical attack

This test was conducted according to the method set out in point 8 of standard UNE EN ISO 10545-13: 1998 'Ceramic tiles-Part 13: Determination of chemical resistance'. The method consists of subjecting the surface of glazed ceramic tiles to a set volume of reagent for a certain time. The samples were classified according to the method described in the standard after rinsing and drying the samples. A(V): no visible effect, B(V): definite change in appearance, C(V): partial or complete loss of the original surface.

Microhardness and fracture toughness

Young's modulus (E) and Berkovich microhardness (HB) were determined by a continuous depth-recording technique.

TABLE II. CHEMICAL ANALYSIS OF THE RAW MATERIALS USED TO PREPARE THE GLAZES (WT%).

	SiO_2	Al_2O_3	B_2O_3	Fe_2O_3	CaO	MgO	Na_2O	K_2O	TiO_2	ZnO	P_2O_5	LOI
Frit	58.4	6.4	3.11	0.07	12.4	2.95	<0.01	4.84	0.03	11.3	<0.01	0.35
Kaolin	48.1	37.0	--	0.78	0.04	0.21	0.01	1.15	0.12	--	0.05	12.66

The unloading data were analysed with a linear fit. Fracture toughness (K_{IC}) was determined from measurements of radial cracks (c) from the Berkovich indentation according to the following equation:

$$K_{IC} = 0.016 \cdot \left(\frac{E}{HB}\right)^{0.5} \cdot P \cdot c^{1.5}$$

Scratch critical load

Scratch critical load (L_C) was determined on a NanoTest system fitted with a Rockwell indenter. Spherical tip radius was 25 μm. Scratches of 1 mm length were made, the load being progressively increased from 0 to 2000 mN. Before and after surface scratching, the indenter probe scanned the surface to be tested, recording the surface profile. This enabled depth changes in the scratched surface to be detected.

3. RESULTS

3.1 Glaze aesthetic characteristics

OPACITY

Figure 1 shows the evolution of the chromatic co-ordinates at 1120 °C with the SSA of the alumina added to the glaze. The dashed lines show the values of the chromatic co-ordinates for the STD glaze. The use of alumina increases L* and reduces a* and b* with respect to the STD glaze, owing to the slight opacifying effect of this raw material.

As alumina SSA increases, the value of L* increases to a peak value at 10 m^2/g and then decreases slightly. The a* and b* co-ordinates decrease as SSA increases up to values around 10 m^2/g, after which stabilisation is observed. These results indicate that raising SSA from 0.3 to 10 m^2/g yields a whiter and more opaque glaze. Higher SSA does not increase glaze opacity.

COLOUR AND GLOSS

Figure 2 depicts the evolution of the whiteness and yellowness indexes at 1120 ºC with the SSA of the alumina introduced into the glaze. The dashed lines show the values of both indexes for the STD glaze. When the SSA increases, the WI values peak at 10 m^2/g, and then decrease slightly, as occurred with the L* co-ordinate in the opacity test. The YI shows an opposite evolution. The evolution in whiteness is due to the variation in opacity as alumina SSA changes. The rise in whiteness, with respect to the STD glaze, is small when AC28 and AC34 aluminas are introduced, and higher with AR308 and AR75 aluminas. This means that aluminas with a high SSA (AR308 and AR75) act as opacifiers and whitening agents.

Raising alumina SSA reduces glaze gloss except for AR75, which displays a value similar to that of AR308 (Figure 3). This means that high SSA aluminas (AR308 and AR75) act as matting agents in this type of glaze, but this is not the case with the high-calcined aluminas (AC28 and AC34).

In conclusion, the tested aluminas can be divided into two groups according to the properties they contribute to the glaze. High SSA aluminas (low-calcined aluminas) give rise to whiter and more opaque glazes than low SSA aluminas (high-calcined aluminas). On the other hand, high SSA aluminas dramatically reduce glaze gloss, while low SSA aluminas hardly modify this. These results match those obtained by other authors [11].

3.2 Glaze microstructure

IDENTIFICATION OF CRYSTALLINE PHASES

Table III summarises the crystalline phases detected in the glazes before firing (U: unfired) and after firing at 1120 °C (F: fired). Kaolinite, stemming from kaolin, was detected in all unfired glazes. Corundum or α-Al_2O_3 was present

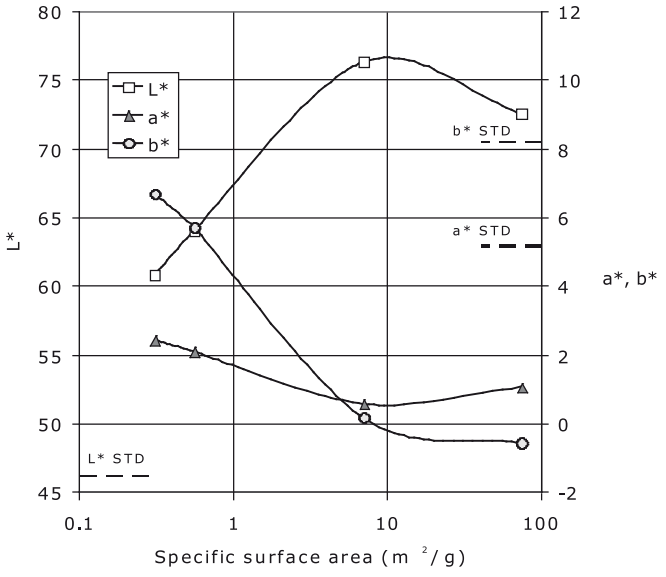

Figure 1. Evolution of L*, a*, and b* co-ordinates with alumina SSA. Glazed tiles without engobe.

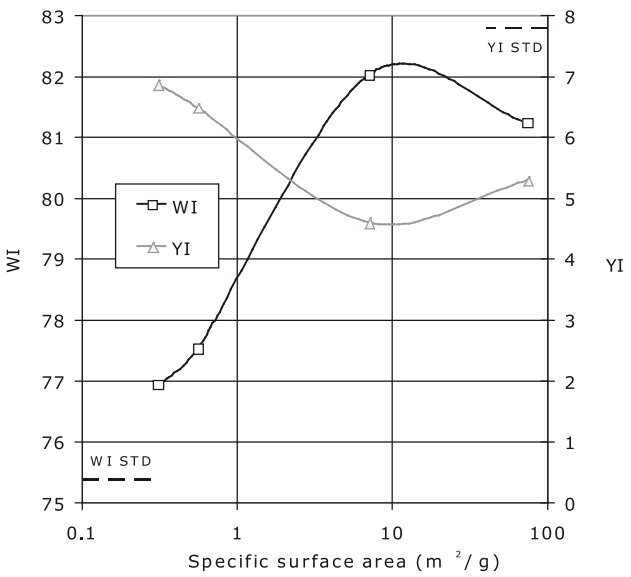

Figure 2. Evolution of WI and YI with alumina SSA. Glazed tiles with engobe.

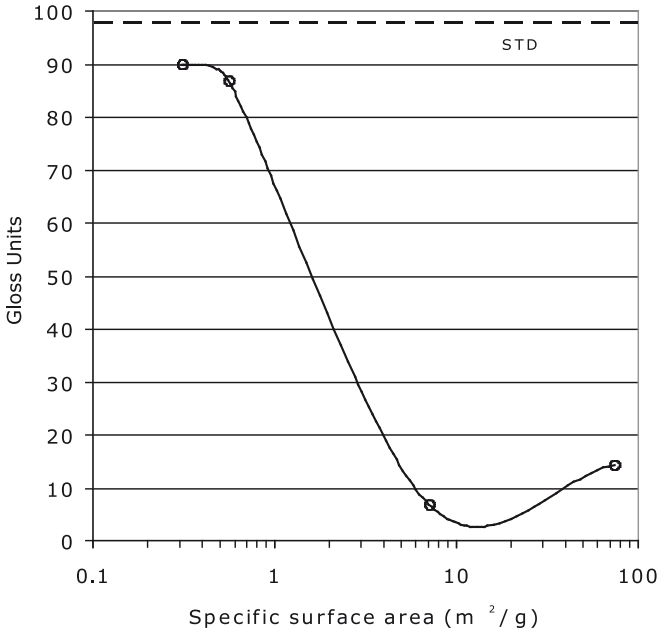

Figure 3. Evolution of gloss with alumina SSA. Glazed tiles with engobe.

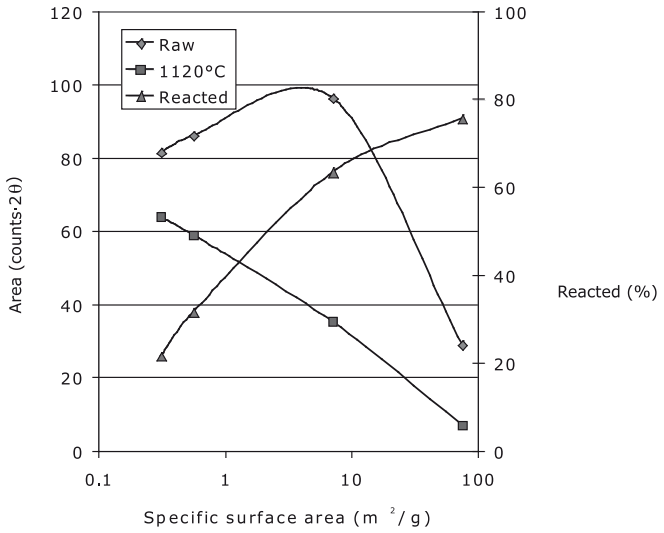

Figure 4. Evolution of corundum peak area with alumina SSA.

in all unfired glazes, except for the STD glaze, because all tested aluminas contained this crystalline phase in different quantities. Diaoyudaoite was also present in the unfired AC34 glaze.

New crystalline phases containing Ca, Zn, and Mg were detected in the fired glazes, due to the reaction between alumina particles and glassy phase stemming from the frit used.

The peak areas of a crystalline phase depend not only on the quantity of this phase in the sample, but also on the crystalline phase itself. As a result, the peak area between two different crystalline phases cannot be compared.

Figure 4 depicts the evolution of the corundum peak area in the glaze with alumina SSA, before and after firing at 1120 °C. It can be observed that the unfired peak area increases slightly in the order AC28, AC34, and AR308, and decreases dramatically in AR75. This is due to the low degree of calcination of AR75. After firing, the corundum peak area decreases with the increase in SSA, which indicates that the corundum particles disappear (by dissolution or formation of new crystalline phases) into the glaze. To establish the quantity of α-alumina that disappears during glaze firing, the following parameter has been calculated:

$$\text{Reacted } \alpha\text{-alumina } (\%) = \frac{\text{Corundum peak area before firing} - \text{Corundum peak area after firing}}{\text{Corundum peak area before firing}} \cdot 100$$

Figure 4 shows that the quantity of reacted or dissolved corundum increases with specific surface area. For this reason, high SSA aluminas are known as 'reactive aluminas'.

Figure 5 shows the crystalline phases detected in the fired glazes. Corundum and anorthite ($CaO{\cdot}Al_2O_3{\cdot}SiO_2$) were the only detected phases in the glazes with low SSA alumina. In the glazes with high SSA alumina, besides corundum and anorthite, gahnite ($ZnO{\cdot}Al_2O_3$) and akermanite ($2CaO{\cdot}MgO{\cdot}2SiO_2$) were also found, the last phase only being detected for AR75 alumina.

The reduction in corundum and the increase in new crystalline phases indicate that alumina reactivity increases with its SSA. The appearance of new crystalline phases during firing means that some changes occur in the chemical composition of the glassy phase (calcium, zinc, and magnesium oxide sequestration), which modify glaze viscosity and, consequently, resulting aesthetic properties (opacity, whiteness, and gloss).

Plotting opacity (L* co-ordinate of the glazed tile without engobe) as a function of the peak area of the main crystalline phases (corundum, anorthite, and gahnite) yields Figure 6. Glaze opacity is observed to increases linearly with the quantity

TABLE III. CRYSTALLINE PHASES DETERMINED BEFORE FIRING (U) AND AFTER FIRING (F) THE GLAZES AT 1120 °C.

Crystalline phases	STD		AC28		AC34		AR308		AR75	
	U	F	U	F	U	F	U	F	U	F
Kaolinite	X		X		X		X		X	
Corundum α-Al_2O_3			X	X	X	X	X	X	X	X
Diaoyudaoite $NaAl_{11}O_{17}$					X					
Anorthite $CaO{\cdot}Al_2O_3{\cdot}SiO_2$				X		X		X		X
Gahnite $ZnO{\cdot}Al_2O_3$								X		X
Akermanite $2CaO{\cdot}MgO{\cdot}2SiO_2$										X

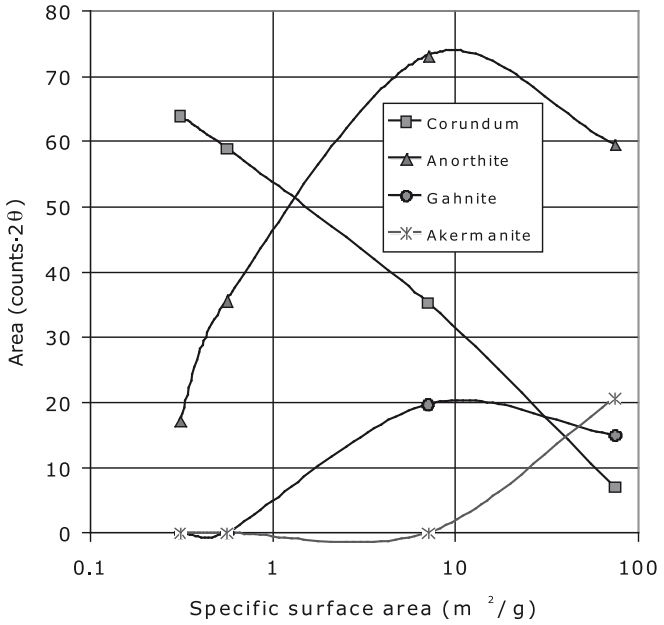

Figure 5. Evolution of crystalline phases (peak area) in the fired glaze with alumina SSA.

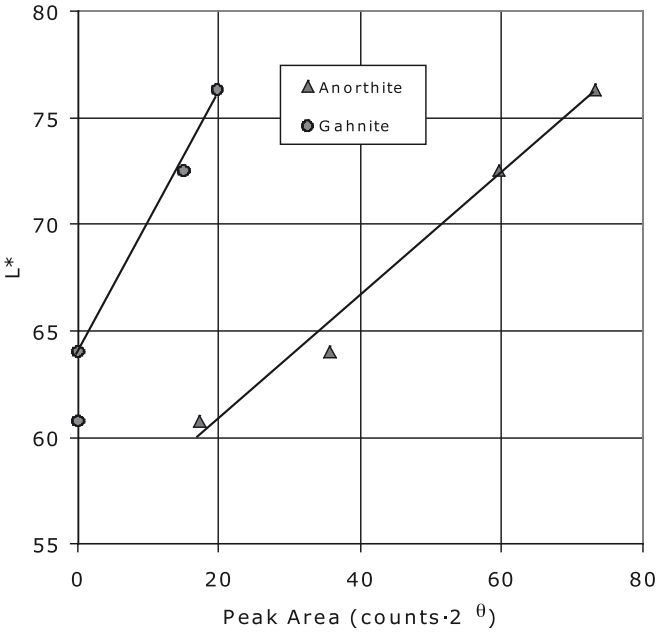

Figure 6. Relationship between opacity and crystalline phase peak area.

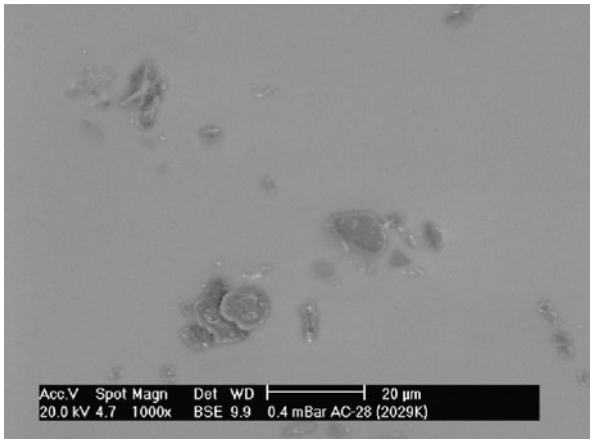

Fig. 7.1. AC28 Glaze.

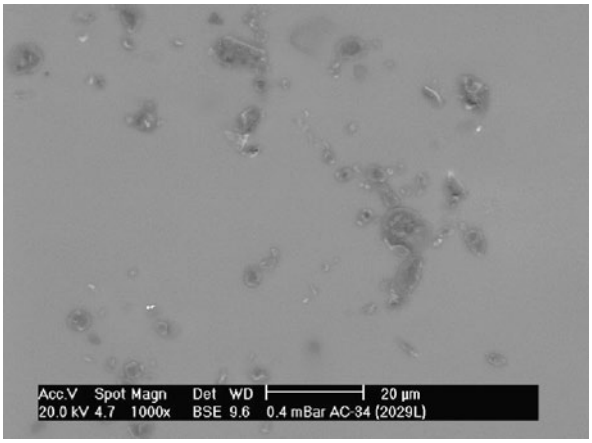

Fig. 7.2. AC34 Glaze.

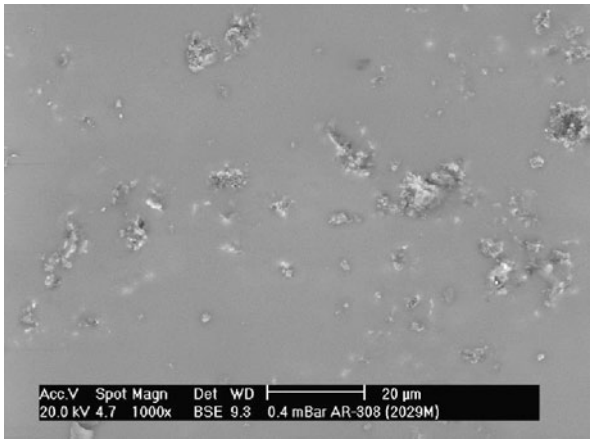

Fig. 7.3. AR308 Glaze.

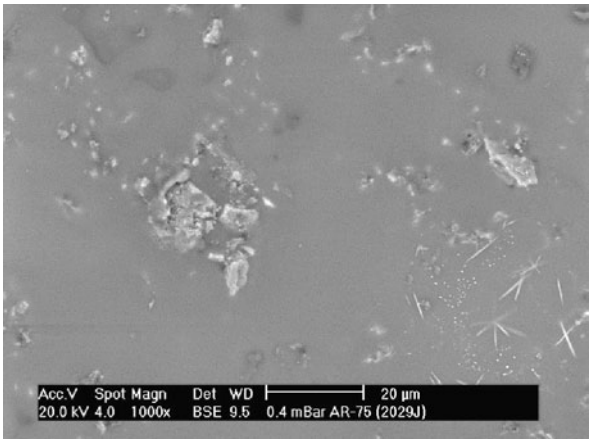

Fig. 7.4. AR75 Glaze.

Figure 7. Micrographs of the surface of the glazed tiles.

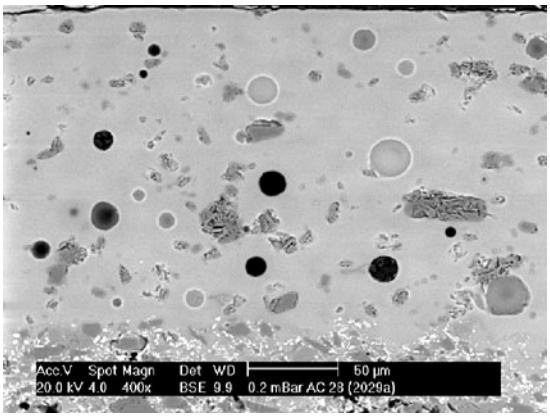

Fig. 8.1. AC28 Glaze.

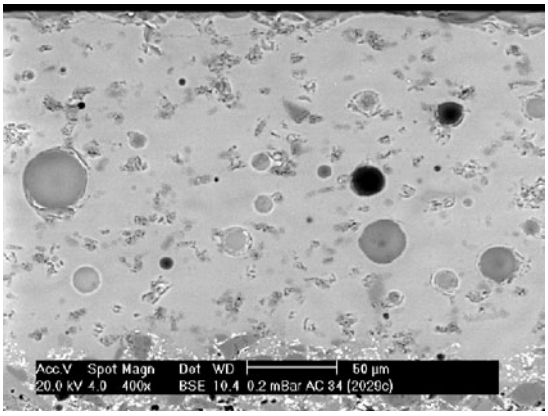

Fig. 8.2. AC34 Glaze.

Figure 8. Cross-sections of the AC28 and AC34 glazes.

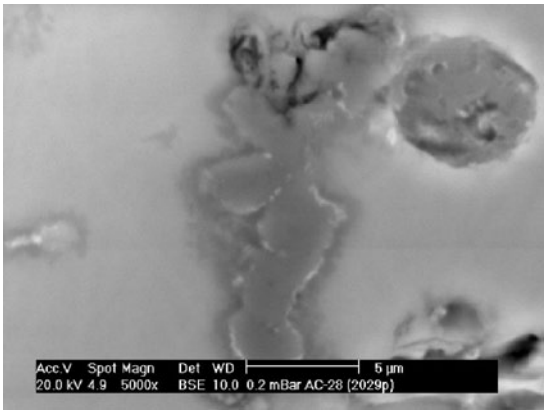

Figure 9. AC34 Glaze. Detail of alumina particles

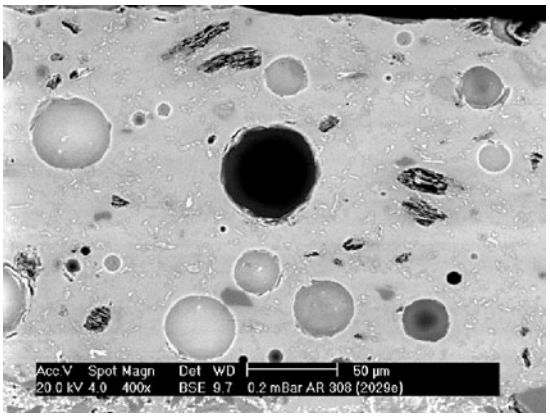

Fig. 10.1. AR308 Glaze.

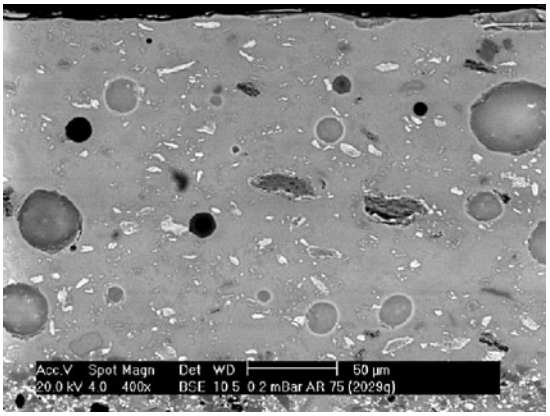

Fig. 10.2. AR75 Glaze.

Figure 10. Cross-sections of the AR308 and AR75 glazes.

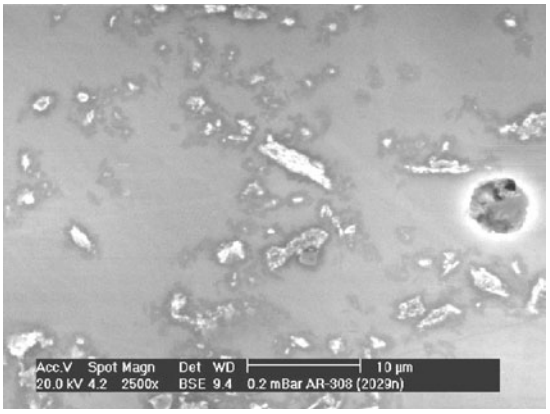

Figure 11. AR308 Glaze detail.

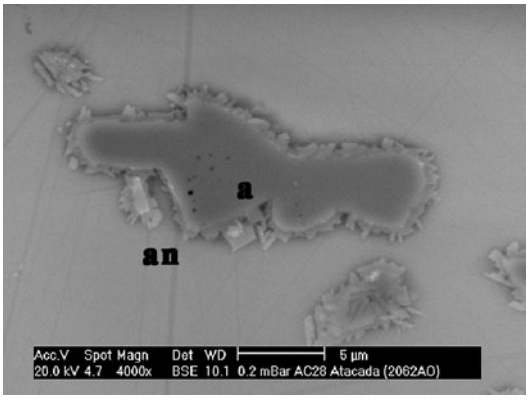

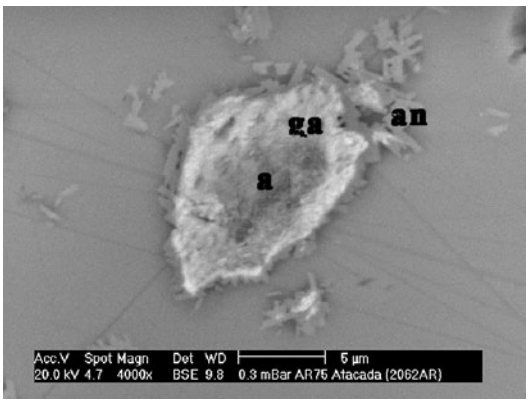

Figure 12. Details of polished glazes after KOH treatment. AC28 Glaze (left) and AR75 Glaze (right)

TABLE IV. GLAZE TECHNICAL PROPERTIES.

Sample	Chemical attack			Mechanical properties		
	HCl 18%	Lactic acid 5%	KOH 100g/l	HB (GPa)	K_{IC} (MPa·m$^{1/2}$)	L_C (mN)
STD	A(V)	A(V)	A(V)	9.4 ± 0.8	1.1 ± 0.1	1230
AC28	A(V)	A(V)	A(V)	10.1 ± 0.6	1.5 ± 0.2	1250
AR75	A(V)	A(V)	A(V)	9.7 ± 0.6	1.3 ± 0.1	High scatter

of new crystalline phases present in the glaze, and to decrease with the corundum content. Opacity is due to light scattering: when the alumina reacts to form new crystalline phases, the number of crystals increases, causing light scattering to increase and producing a more opaque glaze.

The formation of new crystalline phases reduces the quantity of fluxing oxides, such as CaO and ZnO in the glassy phase. This change in glass composition raises viscosity, which prevents surface smoothing, giving rise to a rough surface and a matt appearance [12].

OBSERVATION BY SCANNING ELECTRON MICROSCOPY (SEM)

Figure 7 shows the surface of the glazed tiles. The STD glaze (not shown in the figure) consists of a homogeneous glassy phase containing no crystalline phase. When low SSA aluminas (AC28 and AC34) were added to the glaze (Figs. 7.1 and 7.2), it was observed that alumina particles did not dissolve and hardly reacted with the glassy phase. In glazes with high SSA aluminas (AR308 and AR75, Figs. 7.3 and 7.4), the particles had a lighter colour. EDXA analysis showed that the light colour was due to the reaction of alumina particles with the glassy phase to form gahnite.

Figure 8 shows cross-sections of glazes with low SSA aluminas (AC28 and AC34) observed by SEM. Large alumina particles up to 40 μm long, apparently made up of platelet-like crystals, 3 to 5 μm long, can be observed in Figure 8.1 (AC28). EDXA measurements confirmed that the large alumina particles had not reacted with the surrounding glassy phase.

The alumina particles in Figure 8.2 (AC34) are smaller than those in the AC28 glaze. The glaze with AC34 alumina contains many small individualised alumina particles, 2 to 3 μm long. When these alumina particles were observed at higher magnifications (Figure 9), the alumina particle boundary was observed to be lighter in colour: gahnite had apparently started to form at this point. A dark area appeared around the alumina particle, which analysis suggests could be anorthite.

Figure 10 shows a cross-section of glazes with high SSA alumina (AR308 and AR75). The alumina in the AR308 glaze (Fig. 10.1) had a clearly bimodal particle-size distribution. There were large elongated particles, up to 40 x 15 μm in size. There were also small particles, up to 5 μm long. Small alumina particles had completely reacted to form gahnite. The large alumina particles had reacted to a lesser extent, mainly at their surface, because they exhibited a layer of gahnite. Figure 11 shows an SEM detail of the AR308 glaze displaying light-coloured particles (gahnite) with darker areas around the reacted alumina particles, where anorthite had formed.

Finally, the AR75 glaze (Fig. 10.2) exhibits a similar appearance to that of AR308. There are larger, not completely reacted, alumina particles (dark colour), and small alumina particles that have reacted completely to form gahnite (light colour).

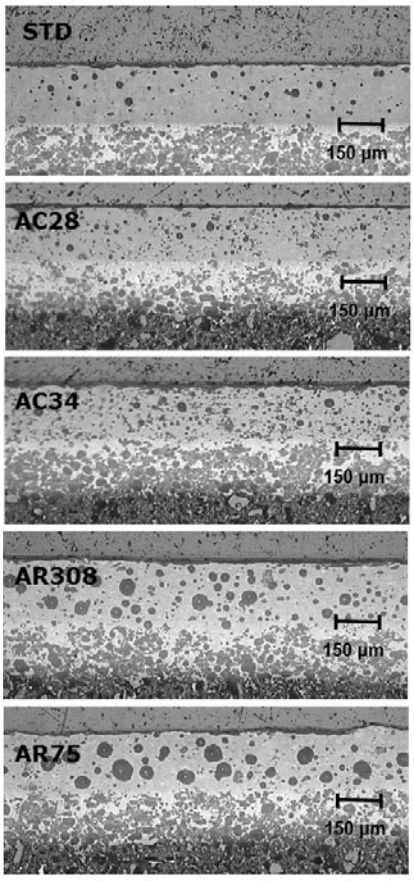

Figure 13. Micrographs of glaze layer cross-sections.

As the anorthite crystals could not be clearly observed by SEM, the surfaces of glazes containing AC28 and AR75 were polished and subjected to alkaline attack by KOH. Figure 12 shows a detail of the resulting surfaces. The potassium hydroxide dissolved the glassy phase, allowing the alumina particles and crystalline phases to surface. The presence of an alumina particle can be clearly observed in glaze AC28 (**a** in Fig 12 left), whose centre has not reacted, surrounded by anorthite crystals (**an**).

In the glaze with AR75, the alumina particle (**a** in Fig 12 right) displays a less reacted central region than the rest, a peripheral zone that corresponds to gahnite (**ga**), and anorthite crystals in the area surrounding the particle (**an**).

The observations conducted suggest that anorthite formation is caused by Al_2O_3 dissolution in the glassy phase surrounding the alumina particles, where the presence of CaO and SiO_2 from the glassy phase favours anorthite crystallisation. Gahnite formation appears to be caused by diffusion of the zinc oxide present in the glassy phase inwards into the alumina particles.

Akermanite was not observed by SEM due to the small quantity of MgO in the frit (2.95 wt%).

The SEM observations show, as already noted above, that the formation of new crystalline species from alumina raises glaze opacity due to the increased surface area, which can produce light diffraction (formation of very small crystals).

GLAZE POROSITY

With a view to determining the evolution of porosity with the degree of alumina calcination, a cross-section of the glaze layers was observed by optical microscope. The resulting photos are shown in Figure 13. Introducing alumina into the STD glaze is observed to increase the number of pores. This is a common effect when refractory particles are present in a melt; these particles hinder proper bubble removal.

In the glazes with AR308 and AR75 alumina, the pores are larger than in the glazes with AC28 and AC34 alumina. The increased viscosity of the glassy phase, when CaO and ZnO are extracted to form new crystalline phases, hinders bubble removal [13][14].

3.3 Glaze technical properties

In this section, tests were only performed with AC28 and AR75 alumina, because these samples are quite representative of the characteristics of the two alumina test groups: high- and low-calcined aluminas. The results are shown in Table IV.

It can be observed that, after chemical attack, none of the samples displayed any change in appearance: all were therefore resistant to chemical attack.

The addition of both aluminas increased fracture toughness in respect of the STD glaze, but did not modify microhardness. The improved toughness, which is more significant for AC28, might be caused by the addition of high-modulus and high-strength particles (alumina) to a low-modulus and low-strength glass matrix, which strengthens the glass matrix, or by the partial dissolution of alumina in the glassy phase [15][16]. The reason that microhardness (HB) did not change with the alumina addition might be because the tests were conducted on an area free of alumina particles.

The average critical load values are also shown in Table IV. No significant difference is observed between the STD glaze and the AC28 glaze. For the AR75 glaze, the results show a great scatter owing to the high surface roughness [17].

4. CONCLUSIONS

This study examines the effect of the degree of alumina calcination on the technical and aesthetic properties of a standard transparent and glossy glaze used in glazed ceramic tile manufacture. The following conclusions can be drawn:

Glaze microstructure

- Alumina particles react during firing with the glaze components (SiO_2, CaO, and ZnO) to form new crystalline phases (anorthite and gahnite). When alumina SSA increases, more new crystalline phases and less α-Al_2O_3 are present in the glaze.
- Anorthite crystallisation is due to alumina diffusion into the glassy phase, while gahnite formation occurs when ZnO diffuses inside the alumina particles.
- Both crystallisations extract CaO and ZnO from the glassy phase, increasing glassy phase viscosity.

Aesthetic properties

- High SSA aluminas provide the glaze with greater opacity and whiteness than low SSA aluminas. This is due to the reaction of low-calcined aluminas to form new crystalline phases during firing.
- Low SSA aluminas produce a slight decrease in glaze gloss. In contrast, high SSA aluminas yield glazes with a matt appearance. This last effect is due to a lack of fluxing oxides in the glassy phase, which increases viscosity.

Technical properties

- An increase in alumina SSA yields a more porous glaze, because bubble removal is hindered when glassy phase viscosity increases.
- No differences in resistance to chemical attack and critical load are detected.
- The addition of alumina increases fracture toughness in the glaze, but does not modify microhardness.

REFERENCES

1. W.H. GITZEN, (ED.) *Alumina as a ceramic material*. Columbus: American Ceramic Society, 1970.
2. Alumina in all its forms. [on line]. [Visited: 2009-07-15] <http://www.specialty-aluminas.alcan.com/gardanne/EVO_WebSpecialtyGlobal.nsf/vwUrl/MondeAlumine_Alumines_VI>
3. K. MINSSEN, Ceramic glaze materials: the top ten list. *Ceram. Eng. Sci. Proc.*, 18(2), 308-319, 1997.
4. A. MORENO; F. NEGRE, Materias primas más relevantes utilizadas en la preparación de esmaltes y engobes cerámicos. In: *I Jornadas sobre materias primas de la industria cerámica (2ª parte). Materias primas para fritas. Materias primas para esmaltes y colores cerámicos. Castellón 22-23 May 1996*.
5. *Tecnología cerámica aplicada: Volume I*. Castellón: Faenza, 2004.
6. R.A. EPPLER, Controlling glaze surface effects. *Adv.Sci.Technol.*, 34, 43-54, 2003.
7. F. CAMPA; F. GINÉS; J. ROBLES, Matting of a transparent porous wall tile glaze by adding alumina. In: *Qualicer 2000: VI World Congress on Ceramic Tile Quality*. Castellón: Cámara Oficial de Comercio, Industria y Navegación, vol. I, 2000, pp. Pos 15-17.
8. E. QUINTEIRO, J.C. CARVALHO; B.A. MENEGAZZO; A.P.M. MANEGAZZO; V.A. SILVA; N.G. SILVA, Comparative study of adding different aluminas to ceramic glazes and engobes. In: *Qualicer 2004: VIII World Congress on Ceramic Tile Quality*. Castellón: Cámara Oficial de Comercio, Industria y Navegación, vol. III, 2004, pp. Pos 143-145.
9. M.F. TOMIZAKI; S. SHINKAI, Influence of the grain size of alumina in the glaze of fast-fired porcelain tiles. *J. Ceram. Soc. Jap., Int. Ed.*, 103(4), 330-334, 1995.
10. E. BOU SOLSONA, *Alternativas al uso del circón como materia prima para preparar recubrimientos vidriados opacos, con el fin de reducir su consumo*. [PhD dissertation]. Castellón: Universitat Jaume I, 2006, pp 109-115.
11. R. LORENZ, L. BOSCARDIN, Study concerning the reactivity of alumina in white body glazes for single firing. *Int. Ceram. J.*, 13(51), 37-39, 1991.
12. E. BOU, M.C. BORDES, C. FELÍU, M.F. GAZULLA, F. FERRER, G. PASIES, Variables that determine the matt appearance of some ceramic floor and wall tile glazes. In: *Qualicer 2002: VII World Congress on Ceramic Tile Quality*. Castellón: Cámara Oficial de Comercio, Industria y Navegación, vol. II, pp. P.GI 349-364.
13. A. ESCARDINO; J.L. AMORÓS; M.J. ORTS; A. GOZALBO; S. MESTRE; J. APARISI; F. FERRANDO; L. SÁNCHEZ. Sintering of ceramic glazes. Effect of composition on resulting glaze porosity. Sintering of ceramic glazes. Effect of composition on resulting glaze porosity. In: 9º *Congreso Mediterráneo de Ingeniería Química*. Libro *de resúmenes*. Barcelona: Fira de Barcelona, 2002, pp. 262.
14. J.L. AMORÓS; M.J. ORTS; A. GOZALBO; A. BELDA; F. SANMIGUEL, F. RODRIGO; V. FERRANDO. Evolution of glaze porosity in firing. Sintering mechanism kinetics. *Ceram. Acta*, 8(3), 5-20, 1996.
15. L. LIMA DIAS; E. QUINTEIRO; A. ORTEGA BOSCHI, Effect of the presence of crystals on glaze wear resistance. In: *Qualicer 2000: World Congress on Ceramic Tile Quality*. Castellón: Cámara Oficial de Comercio, Industria y Navegación, vol. I, 2000., pp. P.GI 17-25.
16. A. SCARDINO, A. MORENO, M.J. IBÁÑEZ, A. BARBA, Relación entre las propiedades mecánicas de vidriados cerámicos y su resistencia al desgaste. *Bol. Soc. Esp. Ceram. Vidr.*, 39(2), 209-214, 2000.
17. M.J. IBÁÑEZ, Scratch test on ceramic tiles. In: *Advances In Nano-Scale Materials Properties Testing using the Nano Test (TM) Birmingham 17-18 December, 2002*.

Recibido: 17-6-10
Aceptado:15-7-10